Applied Meteorology Unit (AMU) Quarterly Report

31 January 2012   First Quarter FY-12   Contract NNK06MA70C

Atlas V launching the Mars Science Laboratory on 26 November 2011 (http://www.spaceflightnow.com/atlas/av028/gallery/index2.html)

In this issue:

Objective Lightning Probability Forecast, Phase IV

Objective Lightning Probability Forecasts for East-Central Florida Airports

Vandenberg AFB Upper-Level Wind Launch Weather Constraints

Applications of Dual-Doppler Radar

Range-Specific High-Resolution Mesoscale Model Setup, Phase I

Launch Support

Dr. Watson and Dr. Huddleston supported the Atlas V launch on 26 November 2011.

This Quarter's Highlights

Ms. Jaclyn Shafer joined the AMU team in December.

The AMU team began work on five tasks for their customers:

- Dr. Bauman and Ms. Crawford are working together on two objective lightning probability tool tasks, one for the Kennedy Space Center/Cape Canaveral Air Force Station (KSC/CCAFS) area and the other for airports in east-central Florida.

- Mr. Wheeler and Ms. Shafer began analyzing sounding data to create a tool that will assist the forecasters at Vandenberg Air Force Base determine the probability of violating specific upper-level wind criteria during launches.

- Dr. Huddleston is conducting a literature review and has interviewed several radar experts to determine the feasibility of using two local Doppler radars to create a dual-Doppler wind field analysis over KSC/CCAFS.

- Dr. Watson began testing high-resolution model configurations for the Eastern Range and Wallops Flight Facility to better forecast a variety of unique weather phenomena and provide forecasters with more accurate depictions of the future state of the atmosphere.

ENSCO

1980 N. Atlantic Ave., Suite 830
Cocoa Beach, FL 32931
(321) 783-9735, (321) 853-8203 (AMU)

Quarterly Task Summaries

This section contains summaries of the AMU activities for the first quarter of Fiscal Year 2012 (October-December 2011). The accomplishments on each task are described in more detail in the body of the report starting on the page number next to the task name.

## Objective Lightning Probability Forecast, Phase IV ([Page 4](#))

Purpose: Develop updated equations with six more years of data and use the National Lightning Detection Network (NLDN) daily lightning flash count across central Florida to determine if the data can be stratified by lightning sub-season instead of calendar month. If the data cannot be stratified by lightning sub-season, the monthly equations will be updated with the new data. The 45th Weather Squadron (45 WS) uses the AMU-developed Objective Lightning Probability tool as one input to their daily lightning forecasts. Updating the logistic regression equations with additional data and different stratifications could improve the lightning probability forecast and make the tool more useful to operations.

Flashes:
1079
5 April 1989
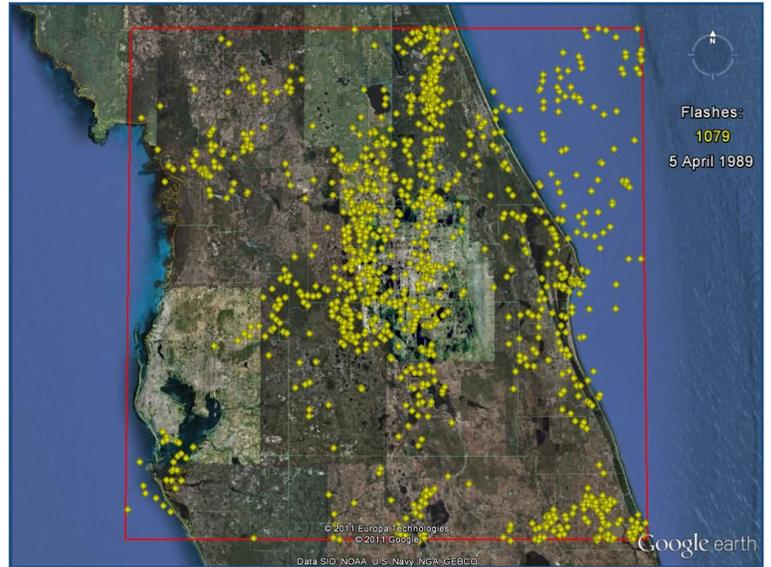
Accomplished: Acquired the NLDN, sounding and Cloud-to-Ground Lightning Surveillance System data. Quality controlled and processed the data to create annual NLDN daily flash counts and calculate the daily flow regimes. Used the NLDN data to determine if lightning sub-seasons could be established and if they could be used operationally in the tool. Met with 45 WS personnel to discuss the results of using the NLDN data to identify the start of the lightning sub-seasons and transition the methodology to operations. Based on the results of this meeting, the task will be completed using a monthly stratification instead of by lightning sub-season.

Objective Lightning Probability Forecasts for East-Central Florida Airports ([Page 7](#))

Purpose: Develop an objective lightning probability forecast tool for commercial airports in east-central Florida to help improve the lightning forecasts during the day in the warm season. The forecasters at the National Weather Service in Melbourne, Fla. (NWS MLB) are responsible for issuing forecasts for airfields in central Florida, and need to make more accurate lightning forecasts to help alleviate delays due to thunderstorms in the vicinity of an airport. The AMU will develop a forecast tool similar to that developed for the 45 WS in previous AMU tasks. The probabilities will be valid for the areas around the airports and time periods needed for the NWS MLB forecast.
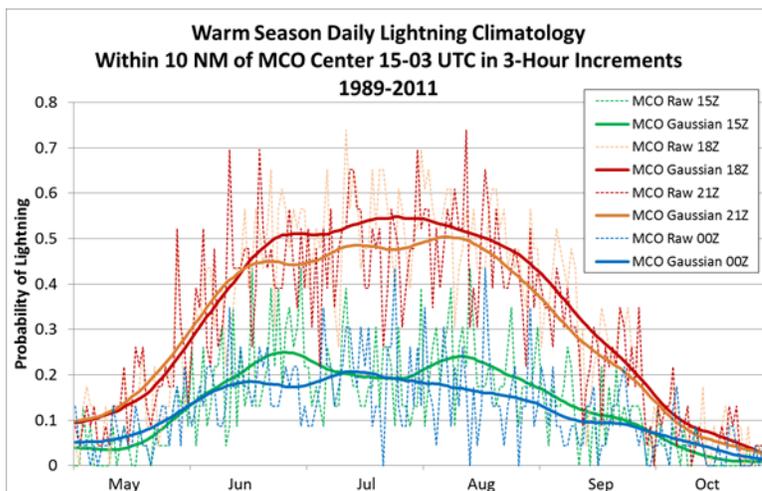

Accomplished: Collected and processed all the data needed for the task. Used the NLDN data to determine lightning occurrence within 10 NM of Orlando International Airport, Melbourne International Airport, and Space Coast Regional Airport in Titusville, Fla. Created the daily lightning occurrence climatologies for each airport.

Quarterly Task Summaries
(continued)

Vandenberg AFB Upper-Level Wind Launch Weather Constraints (Page 9)

Purpose: Develop a tool to determine the probability of violating upper-level wind constraints to improve overall forecasts on the day of launch. This tool will allow the launch weather officers to evaluate upper-level thresholds for wind speed and wind shear constraints specific to Minuteman III ballistic missile operations at Vandenberg Air Force Base (VAFB).

Accomplished: Acquired VAFB soundings from the National Oceanic and Atmospheric Administration Earth System Research Laboratory for the years 1994-2011. Developed scripts to process sounding data and generate output files in the needed format to conduct data analysis.
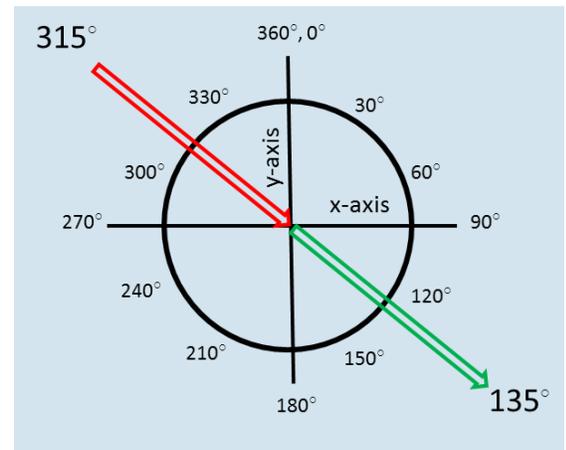
## Applications of Dual Doppler Radar (Page 10)

Purpose: Investigate the feasibility of creating a dual-Doppler capability using the 45 WS and NWS MLB Doppler radars. This would provide a three-dimensional display of the wind field and enhance the forecasters' ability to predict the onset of convection and severe weather. This task involves a literature review and consultation with experts to determine the requirements necessary to establish a dual-Doppler capability. Will also investigate cost considerations and viable alternatives.

Accomplished: Completed the literature search and interviewed experts across the industry. Calculated the geometry of the dual-Doppler area encompassed by the 45 WS and NWS MLB radars, and it appears to be an excellent configuration to provide dual-Doppler winds over Kennedy Space Center and Cape Canaveral Air Force Station. Derived the dual-Doppler equations and completed an outline of the final report. Began investigating cost considerations and possible alternatives.

Range-Specific High-Resolution Mesoscale Model Setup (Page 13)

Purpose: Establish a high-resolution model for the Eastern Range and Wallops Flight Facility to better forecast a variety of unique weather phenomena. Global and national scale models cannot properly resolve important local-scale weather features due to their coarse horizontal resolutions. A properly tuned model at a high resolution would provide that capability and provide forecasters with more accurate depictions of the future state of the atmosphere.

Accomplished: Ran test cases for August 2011 using two preliminary Weather Research and Forecasting (WRF) domain configurations. Preliminary results comparing the WRF and national model forecasts against wind tower observations showed that the national models had better performance.
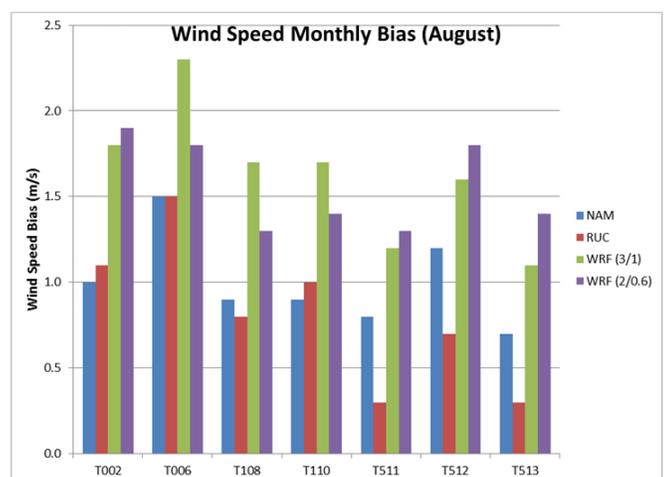
AMU ACCOMPLISHMENTS DURING THE PAST QUARTER

The progress being made in each task is provided in this section, organized by topic, with the primary AMU point of contact given at the end of the task discussion.

SHORT-TERM FORECAST IMPROVEMENT

Objective Lightning Probability Forecast – Phase IV (Dr. Bauman and Ms. Crawford)

The 45th Weather Squadron (45 WS) includes the probability of lightning occurrence in their daily morning briefings. This forecast is important in the warm season months, May-October, when the area is most affected by lightning. The forecasters use this information when evaluating launch commit criteria (LCC) and planning for daily ground operations on Kennedy Space Center (KSC) and Cape Canaveral Air Force Station (CCAFS). The daily lightning probability forecast is based on the output from an objective lightning forecast tool developed in two phases by the AMU that the forecasters supplement with subjective analyses of model and observational data. The tool developed in Phase II consists of a set of equations, one for each warm season month, that calculates the probability of lightning occurrence for the day more accurately than previous forecast methods (Lambert and Wheeler 2005, Lambert 2007). The equations are accessed through a graphical user interface in the 45 WS primary weather analysis and display system, the Meteorological Interactive Data Display System (MIDDS). The goal of Phase III was to create equations based on the progression of the lightning season as seen in the

daily climatology instead of an equation for each month in order to capture the physical attributes that contribute to thunderstorm formation. Five sub-seasons were discerned from the daily climatology, and the AMU created and tested an equation for each. The Phase III equations did not outperform Phase II. Therefore, the Phase II equations are still in operational use. For this phase, the 45 WS requested the AMU make another attempt to stratify the data by lightning sub-season. The AMU will do this by using lightning observations across central Florida from the National Lightning Detection Network (NLDN) instead of the 45th Space Wing Cloud-to-Ground Lightning Surveillance System (CGLSS) data used in Phase III. The lightning season could start anywhere in central Florida, not just locally at KSC/CCAFS as the CGLSS data would show. In the event that lightning sub-seasons cannot be identified, the AMU will create monthly equations with six

more years of data than used in Phase II.

Data

Dr. Bauman and Ms. Crawford collected all the data needed for this task for the period of record (POR) May-October 1989-2011. This includes the NLDN flash data in an area covering central Florida, the CCAFS 1000 UTC soundings (XMR), and the 1200 UTC soundings from Jacksonville (JAX), Tampa (TBW) and Miami (MFL), Fla. They also collected NLDN data for April and November in the POR to observe lightning behavior before and after the defined lightning season of May-October. The NLDN data were provided by the 14th Weather Squadron through Mr. Roeder of the 45 WS and cover the area shown in Figure 1. Mr. Madison of Computer Sciences Raytheon (CSR) provided XMR and CGLSS data, and Ms. Crawford downloaded the soundings for JAX, TBW and MFL from the NOAA Earth System Research Laboratory (ESRL) website (http://www.esrl.noaa.gov/raobs/).

Data Processing

Dr. Bauman wrote scripts in TIBCO Spotfire S+ (TIBCO 2010) statistical analysis software to extract the daily lightning flash counts from the raw NLDN data and export it as Microsoft Excel files. In Excel, he used Visual Basic for Applications (VBA) to write scripts to create annual charts of the daily NLDN flash count for April-November
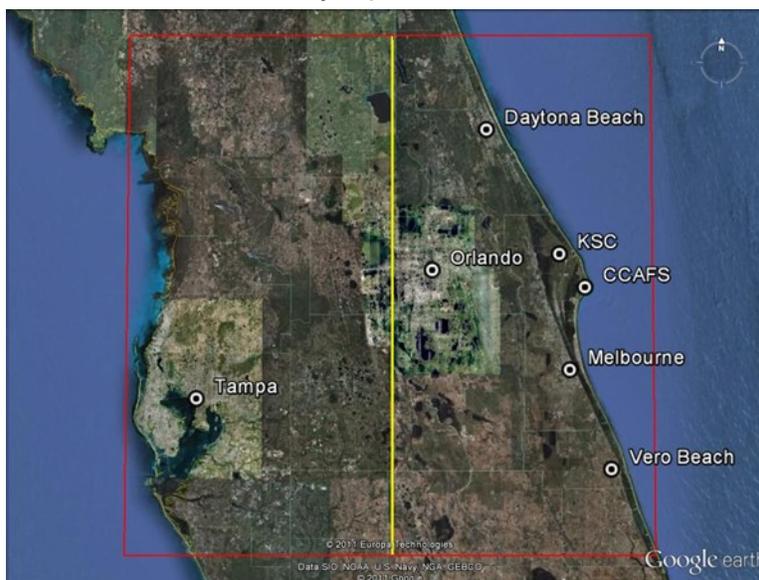

Figure 1. Map of central Florida showing areal coverage (red square) of the NLDN flash count data set. The yellow line is the boundary between east- and west-central Florida.

1989-2011. He also developed VBA scripts in Excel to export the daily NLDN flash locations to Keyhole Markup Language (KML) for display on a map in Google Earth.

Ms. Crawford quality-controlled the XMR sounding data, then determined the flow regimes on each day in the 2010 and 2011 warm seasons using the process described in Lambert (2007). She also calculated the stability indices from the XMR soundings needed as predictors for equation development. The 1989-2009 warm season values were created in earlier AMU tasks.

Ms. Crawford processed the CGLSS data to create the predictand needed for equation development. The predictand is binary and indicates whether lightning occurred within any of the 5 NM warning circles on KSC/CCAFS on each day. She also used the CGLSS data to create the daily climatology and one-day persistence. The daily climatology is the percent of days lightning occurred on each date in the warm season POR. One-day persistence is binary like the predictand, and indicates whether lightning occurred on the previous day.

Lightning Season Start

The approach Dr. Bauman used to determine the start of the lightning season consisted of analyzing the NLDN daily flash count charts to determine if these data correlated with known National Weather Service Melbourne (NWS MLB) east-central Florida wet season start dates (Lascody 2002). If a correlation between the NLDN start/ramp-up of the lightning season can be established with the wet-season start dates, he will continue to look for correlations between the NLDN data and other lightning sub-seasons: lightning (plateau), ramp-down, and post. The sub-seasons would be determined by the increase, plateau, and decrease in the number of flashes on each day, not just whether or not lightning occurred. He would then develop logistic regression equations stratified by lightning sub-season to

predict the probability of lightning for each day. If a correlation cannot be established with the wet season start dates, the 45 WS requested that equations be created for each month as in previous work.

The chart in Figure 2 shows the daily NLDN lightning flash count across central Florida for April-November 1989. The steel blue line shows the number of flashes observed each day while the royal blue line is the 14-day moving average of the daily flashes. The vertical orange and green lines show the 1989 NWS MLB wet season start and end dates for Orlando International Airport (MCO) and Melbourne International Airport (MLB), respectively. The 1989 wet season start date was 28 May for MCO and 6 June for MLB. The chart shows an increase in flash count beginning in April and peaking in July. It would appear that the start of the lightning season across central Florida preceded the start of the wet season at MCO and MLB. Most years in the POR exhibited similar behavior in which the daily NLDN flash count start and ramp-up occurred prior to the wet season start dates.

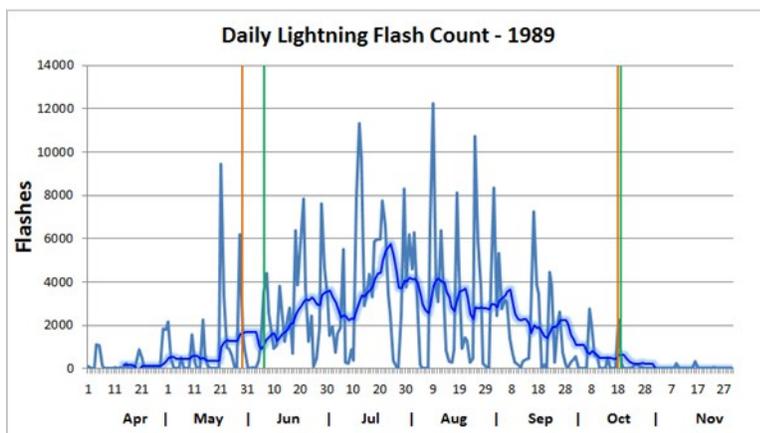After discussing this finding with Mr. Roeder of the 45 WS, Dr. Bauman recommended

Figure 2. Daily NLDN lightning flash count across central Florida for April-November 1989. The steel blue line shows the number of flashes observed each day and the royal blue line is the 14-day moving average of the daily flashes. The vertical orange and green lines show the 1989 NWS MLB wet season start and end dates for Orlando (MCO) and Melbourne (MLB), respectively.

considering two additional stratifications to try and account for the difference: (1) limit the areal coverage of the NLDN data to east-central Florida and (2) eliminate any lightning days due to influences from synoptic weather patterns such as cold fronts that will sometimes penetrate into central Florida as late as May.

Dr. Bauman developed a VBA script to convert Excel NLDN flash data into KML format to display each flash on a map of central Florida in Google Earth. He was then able to visually inspect each day's NLDN strike locations. The map in Figure 3 shows an example of this display for 5 April 1989. By reviewing similar
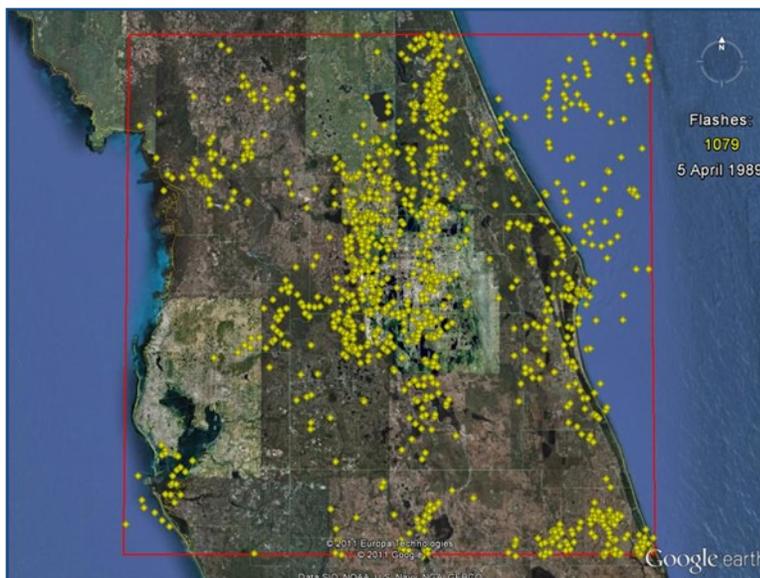

Figure 3. The NLDN flashes in central Florida (see Figure 1) for 5 April 1989. Each yellow dot represents one cloud-to-ground lightning flash. On this day there were 1,079 flashes across central Florida within the area bounded by the red lines.
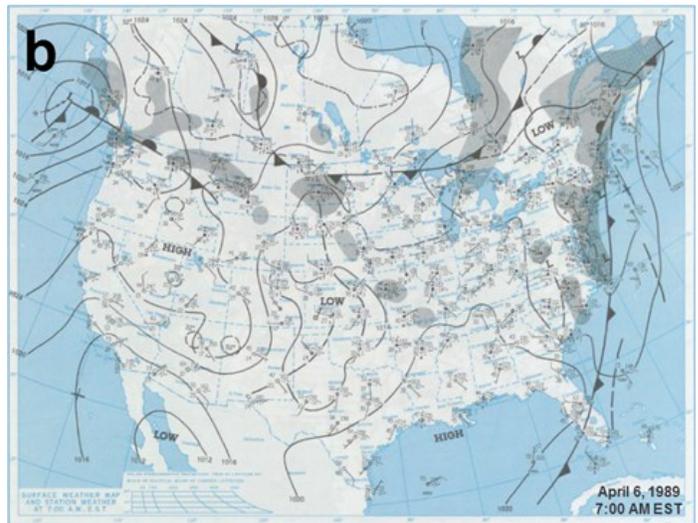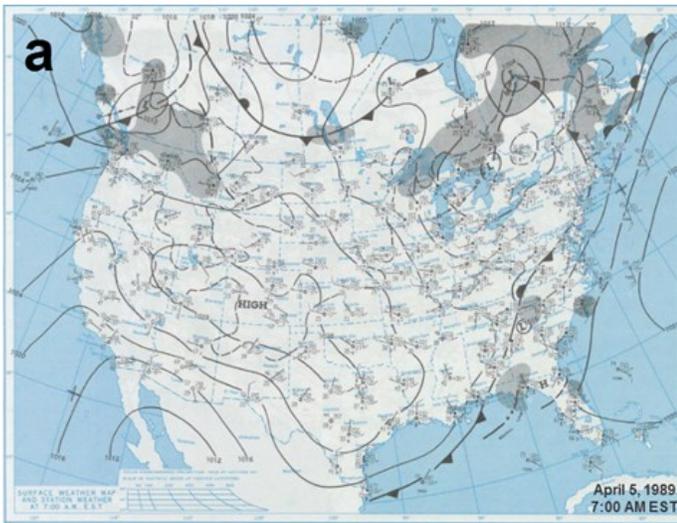
Figure 4. The NOAA daily weather maps (NOAA 2011) from (a) 5 April 1989 and (b) 6 April 1989 showing surface synoptic-scale weather systems.

NLDN maps for April and May of all years in the POR, Dr. Bauman discovered it was not uncommon for lightning to occur early in the warm season as in Figure 3, and not be confined to the east or west half of the state as is more typical under prevailing westerly or easterly flow warm season regimes. However, as the warm season progressed, there were clear divisions between east and west coast daily NLDN events dependent on the flow regime. Therefore, Dr. Bauman reduced the NLDN data set to flashes only occurring in east-central Florida, which covered the eastern half of the red square in Figure 1. However, his further analysis revealed that reducing the NLDN events to east-central Florida did not explain the non-correlation of the beginning of lightning flash count ramp-up with the NWS MLB wet season start dates.

To account for synoptic weather pattern influences other than the warm season peninsular flow regimes, such as low pressure systems and fronts, Dr. Bauman reviewed all April and May daily weather maps (NOAA 2011) for days with NLDN flashes in central Florida to see if these events could be eliminated from the data set. As an example of a synoptic weather system influence, the daily weather maps for 7:00 AM EST (1200 UTC) on 5 and 6 April 1989 are shown in Figure 4. On 5 April, a cold front was draped across the southeast United States

and a pre-frontal squall line was located in north Florida. By 7:00 AM EST on 6 April, the cold front was located just south of central Florida. It is highly likely that this cold front and/or it's associated pre-frontal squall line was responsible for the NLDN flashes shown in Figure 3. Therefore, the NLDN flashes on 5 April were eliminated from the data set. This methodology resulted in elimination of most NLDN flash days in April and many in May throughout the POR resulting in a better correlation between the NLDN-based lightning season and NWS MLB wet season start dates.

The daily weather maps did not always show lows or frontal systems in the area on days with lightning in April and May, so Dr. Bauman could not conclude that these systems were the cause of the lightning. He did not eliminate these days from the data set. Since not all days with NLDN flashes could be eliminated based on synoptic patterns, determining the start/ramp-up of each lightning season in the POR still had some level of subjectivity. Figure 5

shows the same time period as Figure 2 except it includes only NLDN flashes from east-central Florida with the synoptic weather system influenced flashes removed. Hence, the 1989 east-central Florida lightning season started within a week of the NWS MLB wet season start at MCO.

Over the entire POR, the median NLDN flash count ramp-up started six days prior to the mean MCO/MLB wet season start dates. The earliest NLDN start/ramp-up was 21 days prior to wet season start (1999) and the latest was 3 days after (1996 and 2007). In 65 percent of the years (15 of 23) the start dates were within 7 days of each other. Lascody (2002) notes that in determining the start of the wet season, "It must be stated that a purely objective analysis is not possible since the exact onset of the Wet Season is difficult to determine in some years." Given the subjectivity in determining both the wet sea-
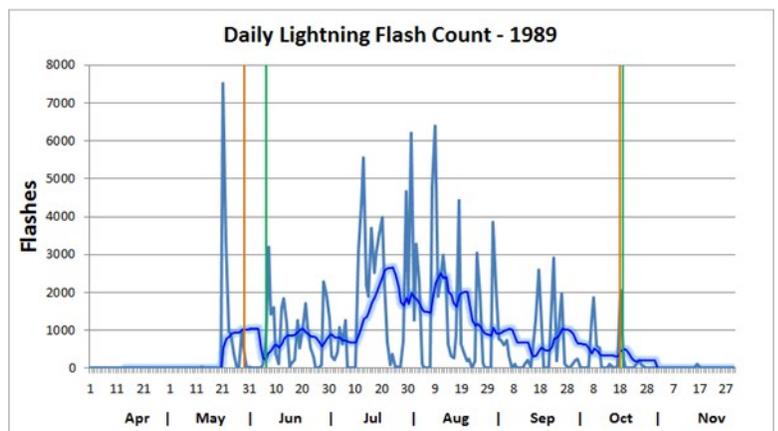

Figure 5. As in Figure 2, but for the east-central Florida region and with NLDN flashes due to synoptic frontal systems removed.

son start and NLDN start/ramp-up and the data presented, it appears there is a correlation between the wet season method and the NLDN method.

Lightning Sub-Season Stratifications

With a correlation established between the NLDN flash count start/ramp-up dates and the NWS MLB wet-season start dates, Dr. Bauman looked for correlations between the NLDN data and other proposed lightning sub-seasons: lightning (plateau), ramp-down, and post. Just as determining the start of the lightning season using the NLDN data was subjective, so was determining sub-seasons. In examination of the annual charts of daily flash count, Dr. Bauman observed there were often multiple sub-seasons of the same type. For example, in Figure 6, it appears there were two ramp-up sub-seasons in 1999 followed by a relatively consistent flash count (plateau) from mid-June through early September, a ramp-down sub-season from mid-September to mid-October, and then a post lightning sub-season. In a second example from 2004 (Figure 7), after the ramp-up, there were two distinct consistently high lightning flash count periods (plateaus) with a lull in lightning flash count from mid-July through early August followed by a ramp-down sub-season and post lightning sub-season.

A question that surfaced while assessing the sub-season stratifications was how the operational forecasters would be able to declare the lightning season start and the sub-seasons in real-time in order to know which equation to use in the tool. Since it was subjective and somewhat difficult to make those determinations using climatological data, Dr. Bauman consulted with Ms. Crawford and Mr. Roeder on how to address this issue. They decided to present the findings to the 45 WS personnel who would use the tool. The discussion led to a consensus that it would be difficult for the forecasters to determine the lightning sub-seasons in real-time using NLDN data. Therefore, Dr. Bauman will proceed with this task

Figure 6. As in Figure 5, but for 1999 and with the lightning sub-seasons highlighted by red brackets and text describing each.
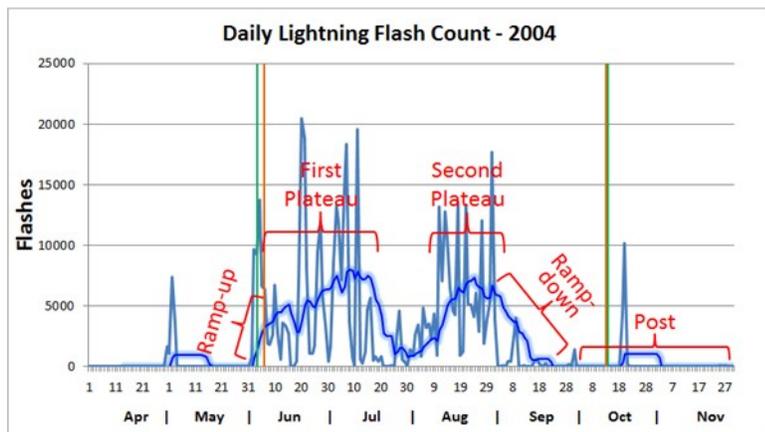
Figure 7. As in Figure 6, but for 2004.

using monthly stratifications to develop the new equations.

For more information contact Dr. Bauman at bauman.bill@ensco.com or 321-853-8202, or Ms. Crawford at crawford.winnie@ensco.com or 321-853-8130.

Objective Lightning Probability Forecasts for East-Central Florida Airports (Ms. Crawford and Dr. Bauman)

The forecasters at the National Weather Service in Melbourne, Fla. (NWS MLB) are responsible for issuing weather forecasts to several airfields in central Florida. They identified a need to make more accurate lightning forecasts to help alleviate delays due to thunderstorms in the vicinity of an airport. Such forecasts

would also provide safer ground operations around terminals, and would be of value to Center Weather Service Units serving air traffic controllers in Florida. To improve the forecast, the AMU was tasked to develop an objective lightning probability forecast tool for the commercial airports in east-central Florida for which NWS MLB has forecast responsibility. The resulting forecast tool will be similar to that developed by the AMU for the 45 WS in previous tasks (Lambert and Wheeler 2005, Lambert 2007). The lightning probability forecasts will be valid for the time periods and area around each airport needed for the NWS MLB forecasts in the warm
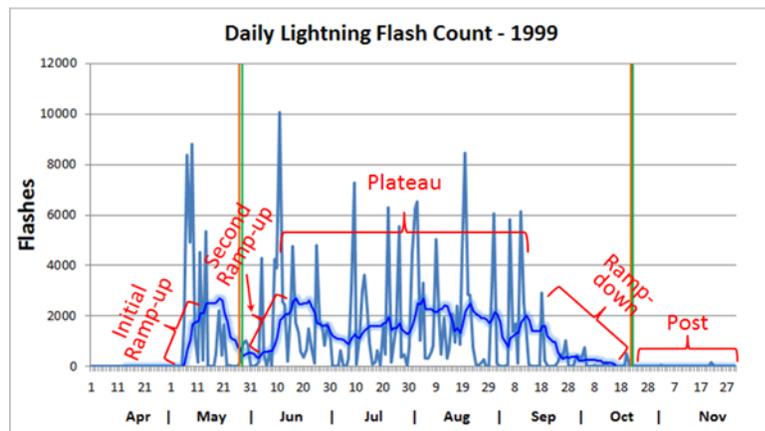
season months, defined as May-October.

Data Preparation

The lightning probability forecasts will be valid for the area within 10 NM of the airport centers and during four three-hour segments in the period 1500-0300 UTC (1100-2300 EDT) to be consistent with the NWS MLB required forecast parameters. They requested equations for MCO be developed first, followed by MLB and then Space Coast Regional Airport (TIX) in Titusville, Fla., time permitting. Ms. Crawford will use the same data in this task as used in the Objective Lightning Probability Tool

Phase IV task described previously, except for the CGLSS data. The range of CGLSS does not include the commercial airports for which NWS MLB makes forecasts.

Ms. Crawford processed the NLDN data and created the predictand, the daily climatology and one-day persistence. The predictand is binary and indicates whether lightning occurred within 10 NM of the airfield center during each three-hour time period. The daily climatology is the percent of days lightning occurred on each date and each three-hour period in the warm season POR. One-day persistence is also binary, and indicates whether lightning occurred on the previous day in each three-hour period.

Once Ms. Crawford developed the scripts to create the predictands climatology and persistence for one station, the time to create the values for all three stations was minimal. Figures 8-10 show the daily climatologies for the four three-hour time periods at each of the stations. These values were calculated using the same 14-day Gaussian smoothing algorithm described in Lambert (2007). For MCO (Figure 8), farther from the coast than the other two stations, the values for 18-2100 UTC and 21-0000 UTC are similar as are the values for 15-1800 UTC and 00-0300 UTC. For MLB (Figure 9) and TIX (Figure 10), the values for 18-2100 UTC are highest, and the time periods before (15-1800 UTC) and after (21-0000 UTC) have values that are more similar. This may show a ramp up and down of lightning occurrence at these two stations as the sea breeze forms close to the coast in the late morning/early afternoon and moves inland in the afternoon, creating higher values for MCO during the mid- and late-afternoon periods.

Data Stratification

The stratification used in this task depended on the stratification used in the Objective Lightning Probability Tool Phase IV task discussed previously. The stratification used in that task would be used in this task. After in-depth analysis and testing as described previously in this report, Dr. Bauman and Ms. Crawford concluded that determining lightning sub-seasons was a difficult and subjective task that would not be practical, and likely not possible, operationally. Therefore, they will stratify the data by month. Dr. Bauman and Ms. Crawford informed the 45 WS and NWS MLB of the results and they agreed to the monthly stratification.

For more information contact Ms. Crawford at 321-853-8130 or crawford.winnie@ensco.com, or Dr. Bauman at 321-853-8202 or bauman.bill@ensco.com.
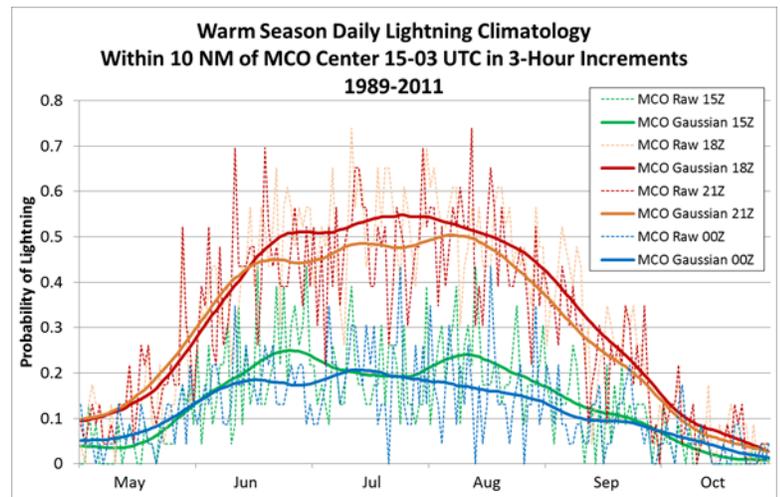

Figure 8. The daily raw and Gaussian-smoothed lightning climatology at MCO for the three-hour periods 15-1800, 18-2100, 21-0000, and 00-0300 UTC. The time values in the legend indicate the beginning of the time period.
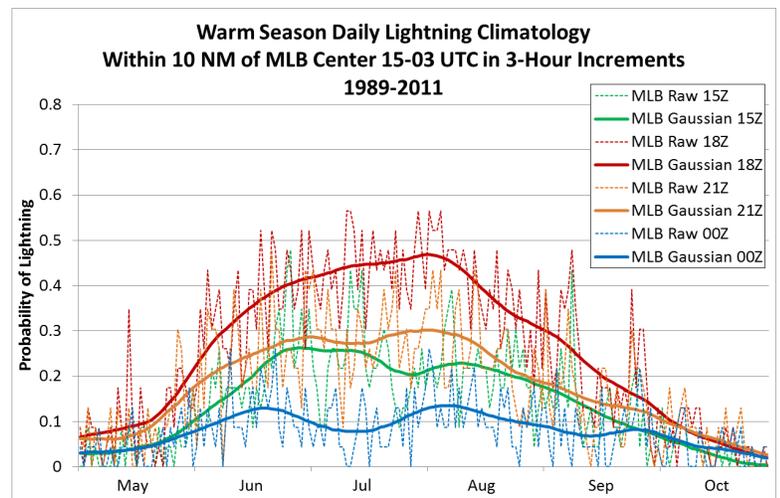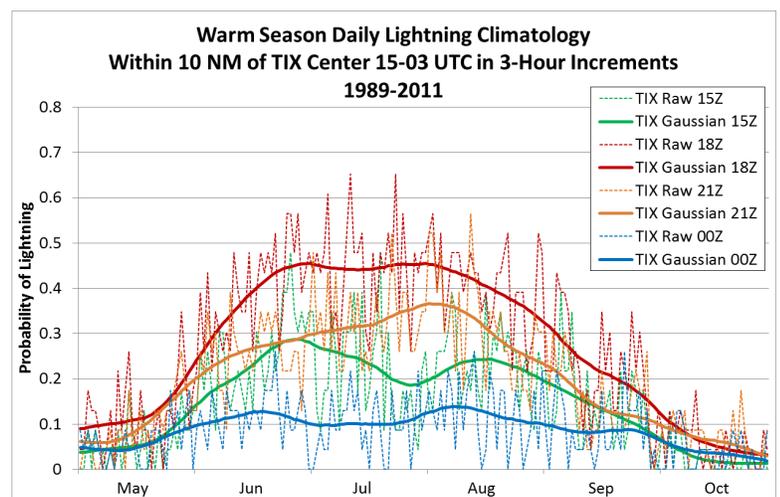

Figure 9. Same as Figure 8 but for MLB.

Figure 10. Same as Figure 8 but for TIX.

Vandenberg AFB Upper-Level Wind Launch Weather Constraints (Ms. Shafer and Mr. Wheeler)

The 30th Weather Squadron (30 WS) provides comprehensive weather services to the space program at Vandenberg Air Force Base (VAFB) in California. One of their responsibilities is to monitor upper-level winds to ensure safe launch operations of the Minuteman III ballistic missile. The 30 WS tasked the AMU to analyze upper-level thresholds for wind speed and shear constraints specific to this launch vehicle using historical data collected at VAFB. The result will be a tool that will assist the 30 WS forecasters in determining the probability of exceeding specific wind threshold values, increase the accuracy of determining the probability of violation, and improve the overall forecast.

Data Acquisition

The ideal data to use for this task would be the soundings collected through the Automated Meteorological Profiling System (AMPS) at VAFB. In their initial proposal for this task, the 30 WS expressed concern about being able to supply this data set to the AMU. Due to limitations of their AMPS system, it would take considerable resources to put the data in a format that could be used in the task. Mr. Tyler Brock of the 30 WS sent a sample AMPS file to Mr. Wheeler in a readable text format. However, the file had no header information identifying which variables were listed, and it was difficult to discern the variables from the values.

To circumvent these issues, Mr. Roeder of the 45 WS suggested using the Range Reference Atmosphere (RRA) data for VAFB. The RRA contains the monthly means and standard deviations of the sounding variables every 0.25 km (~820 ft) using soundings collected in the years 1990-2001 (https://bsx.edwards.af.mil/weather/rcc.htm).

Assuming the variable values were normally distributed, Mr. Wheeler used the means and standard deviations in an Excel formula to calculate the probabilities of exceeding the desired thresholds. The probabilities he calculated never exceeded 1%, and were most often much closer to 0%. He determined that this would not be useful information for the 30 WS.

Mr. Wheeler met with the AMU team, and they decided that useful results would more likely be found by using individual soundings. He determined the VAFB soundings were available in the ESRL archive and in a format that can be easily processed. Mr. Wheeler downloaded VAFB soundings from the NOAA ESRL site (http://www.esrl.noaa.gov/raobs/) for the years 1994-2011. At this point, Ms. Shafer started work on the task so Mr. Wheeler could work on other AMU tasks.

Current Tool

Mr. Tyler Brock of the 30 WS provided Ms. Shafer with an Excel spreadsheet containing the current 30 WS tool for calculating wind shear and determining the likelihood of violation of specific upper-level wind constraints. She examined the contents of the file to determine how the values were calculated; it is important the final tool use the same equations as those used by the 30 WS for consistent operational results. Ms. Shafer discovered some errors in the current 30 WS tool and informed Mr. Brock of the inconsistencies.

The current tool references an incorrect column in the worksheet when calculating the 1,000-ft wind shear and the X (east-west) and Y (north-south) wind components are miscalculated. As an example, if the wind direction is northwest at 315°, the wind is blowing towards 135°. This is represented graphically in Figure 11 by a green vector beginning at the origin (x and y = 0) and pointing toward the southeast. The wind vector is in the bottom right quadrant, resulting in a positive x component and negative y compo-

nent. The AMU calculations reflect these signs while the current 30 WS tool shows the opposite. Ms. Shafer modified the existing references and calculations in the 30 WS tool to correct these issues. To confirm the new calculations were correct, she compared their output to those of the original 30 WS tool using sounding data provided by the 30 WS. Ms. Shafer informed Mr. Brock of the corrections made, and he agreed these changes could have made an impact on past operations. He stated these adjustments will improve their process in the future and provide additional confidence when reporting launch weather status.
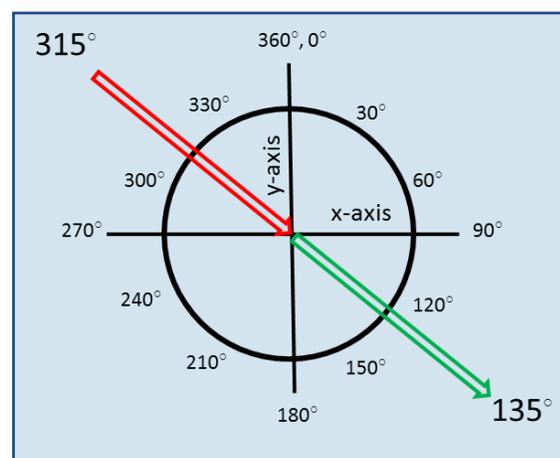

Figure 11. Graphical representation of a northwest wind.

Data Processing

Ms. Shafer completed collecting the VAFB soundings from the NOAA ESRL database and modified existing scripts to import the sounding data into S+ for data analysis. She wrote another script to filter out the sounding data needed for the task requirements and created monthly data files for the wind constraints.

In order to determine the probability of violating each wind constraint, the data needed to be interpolated to the 1,000-ft height levels. Ms. Shafer wrote a Perl script to add the required 1,000-ft levels to each sounding that will be used to analyze the data as necessary.

Contact Ms. Shafer at 321-853-8200 or shafer.jaclyn@ensco.com for more information.

INSTRUMENTATION AND MEASUREMENT

Applications of Dual-Doppler Radar (Dr. Huddleston)

When two or more Doppler radar systems are monitoring the same region, the Doppler velocities can be combined to form a three-dimensional wind vector field. Such a wind field allows a more intuitive analysis of the airflow, especially for users with little or no experience in deciphering Doppler velocities (Bousquet, 2004). A real-time display of the wind field could assist fore-casters in predicting the onset of convection and severe weather. The data could also be used to initialize local numerical weather models. Two Doppler radars are in the vicinity of KSC and CCAFS: the 45 WS RadTec 43/250 radar and NWS MLB Weather Surveillance Radar 88 Doppler (WSR-88D) radar. The 45 WS, NWS MLB and NASA customers tasked the AMU to investigate the feasibility of establishing dual-Doppler capability using these two systems. This task will consist of a literature review and consultation with experts to determine geometry, methods, techniques, hardware and software requirements necessary to create a dual-Doppler capability. The AMU will also investigate cost considerations and viable alternatives.

Dual-Doppler Equations

To facilitate complete understanding of dual-Doppler synthesis and to determine the technical information requirements, Dr. Huddleston derived the dual-Doppler equations to determine how to find the three components of wind velocity from the equation of continuity and radial velocity data collected by two Doppler radars (Armijo, 1969). She will make the derivations available in the Appendix of the final report for the interested reader. She compiled them from a combination of the methods of Armijo (1969), Obrien (1970), Lhermitte and Miller (1970), and Carey (2005). The geometry of the radial
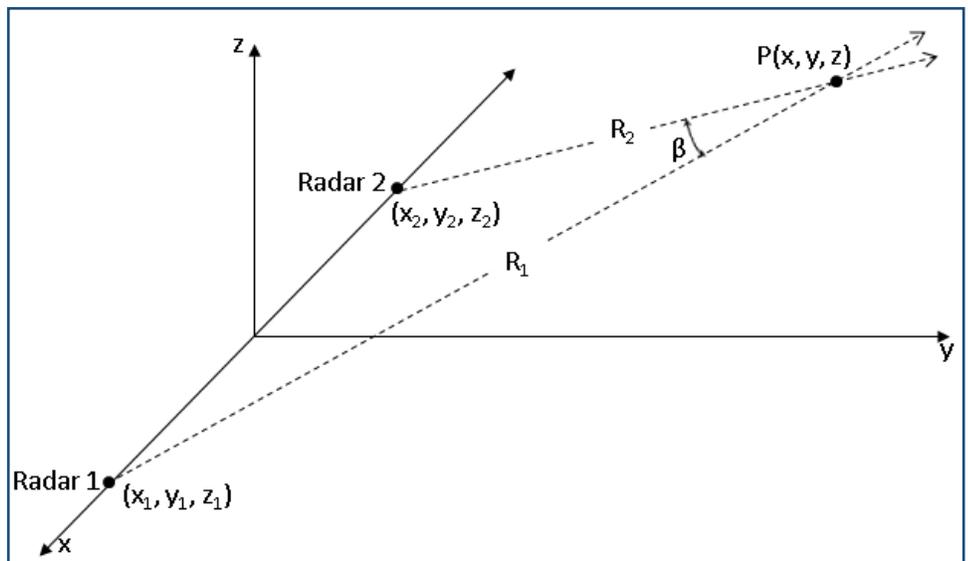
Figure 12. The geometry of the radial distance between radars and a point in space. The target point of the radars is at P(x, y, z), and β is the angle between radar beams at P. Radar 1 is at point (x_1, y_1, z_1) and radar 2 is at point (x_2, y_2, z_2). Adapted from Figure 9.3 in Doviak and Zrnic (1993).

distance between two radars and a point in space is shown in Figure 12. The typical beam geometry for a single radar is shown in Figure 13.

Dual-Doppler Area Geometry

When planning a dual-Doppler capability, the specific area of interest must be studied to determine if the locations of the radars will allow an accurate wind field determination. Dual-Doppler coverage depends on

- The minimum spatial resolution needed to resolve the weather phenomena of interest,
- The largest acceptable error in horizontal velocity, and
- The distance between the radars (Davies-Jones, 1979).

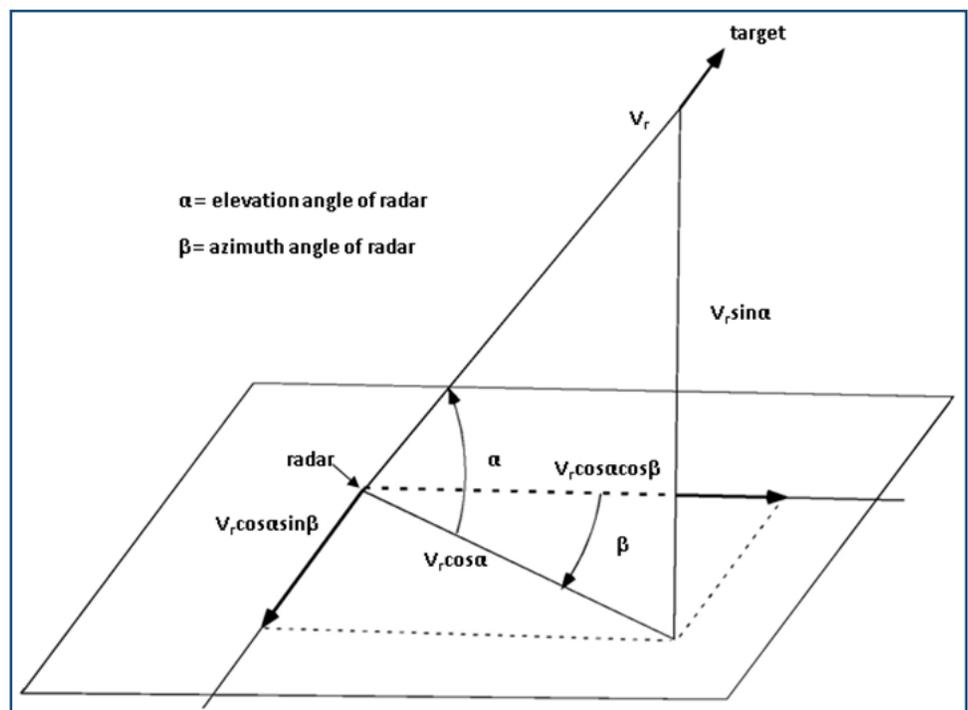The optimal beam crossing angle, that will provide the most accurate wind synthesis is 90° (Beck 2004).

Figure 13. The typical beam geometry for a single radar. Adapted from Figure 6.2 in Rinehart (2004).

To begin the analysis, unit vectors of the two radial velocities intersect angle, β (Davies-Jones, 1979, Friedrich and Hagen, 2004). Using the schematic in Figure 12 as an example, β is the angle between R_1 and R_2 at P. The error variances

$$\sigma_u^2 \quad \text{and} \quad \sigma_v^2$$

of u and v, the velocity components in the x and y directions, are related to the Doppler mean velocity error variances of the two individual radars

$$\sigma_1^2 \quad \text{and} \quad \sigma_2^2$$

by (Davies-Jones, 1979):

$$\frac{\sigma_u^2 + \sigma_v^2}{\sigma_1^2 + \sigma_2^2} = \csc^2 \beta$$

Experience at the National Severe Storms Laboratory (NSSL) has shown that a β of 30° or greater is adequate for accurate wind synthesis (Davies-Jones, 1979). In any β of less than 30° or greater than 150°, a large component of both beams is oriented in the same direction. This will cause large errors in the velocity components derived from the dual-Doppler wind synthesis.

Dr. Huddleston calculated the beam crossing angle between the 45 WS and the NWS MLB radars for launch complexes 17A (Figure 14) and 41 (not shown) on CCAFS. The beam crossing angles for these two locations are 67.9° and 52.2°, respectively, both within the 30° to 150° range recommended by Davies-Jones (1979).

The spatial resolution of the dual-Doppler coverage area is related to the baseline, or horizontal distance between two radars. Davies-Jones (1979) and Friedrich and Hagen (2004) proposed that the optimal distance between two radars would range between 23.2 NM (43 km) and 43.7 NM (81 km). Examination of Figure 14 shows that the baseline between the 45 WS and NWS MLB radars is 23 NM (42.6 km), at the low end of the optimal separation distance.

The beam crossing angles and the baseline of the 45 WS and NWS

Figure 14. The beam crossing angle (67.9°) between the 45 WS and NWS MLB radars for launch complex 17A on CCAFS.

MLB radars makes them ideally suited for a dual-Doppler capability. The next step is to calculate the total coverage area of the dual-Doppler analysis. Davies-Jones (1979) and Friedrich and Hagen (2004) show that the total coverage area is the intersection of the area (A_1) defined by the upper limits on velocity error variance (Figure 15) and the area (A_2) defined by the maximum range of the radars (Figure 16).

The area A_1 is made up of two circular areas called dual-Doppler lobes. In the formula for A_1 as given by (Davies-Jones, 1979) and shown in Figure 15, d is half of the baseline (23 NM/2 = 11.5 NM) and β is the minimum beam crossing angle in radians (π/6 rad or 30°). In the formula for A_2 in Figure 16, R is the maximum range of the radars. The dual-Doppler coverage area is defined as the area common to both A_1 and A_2 (Davies-Jones, 1979):

$$A_{12}(\beta, R) = A_1(\beta) \cap A_2(R).$$

Dr. Huddleston calculated A_1 for the 45 WS and the NWS MLB radars (Figure 17). She has not yet calculated A_2 and A_{12}.

Software

There are several options to collect, edit, synthesize and display dual-Doppler data sets. The 45 WS currently uses the IRIS software package by Vaisala to display their radar data. IRIS software has an add-on product for multiple Doppler radar capability called NDOP that can ingest WSR-88D data. The license includes the ability to make mosaics, or composites, of radar products from multiple sites. The list cost is $16,000.

A variety of freeware packages are available from the National Center for Atmospheric Research (NCAR) for processing raw radar data, but these packages have the disadvantage of not having thorough documentation and stringent configuration control to be certified for 45 WS use.

In any case, a data line must be installed in the 45 WS to enable the receipt of NWS MLB raw radar data to use in the dual-Doppler synthesis. This will likely be costly and time-consuming. Dr. Huddleston will ask the 45 WS to get a cost estimate of purchasing the software, installing the data line, testing, training, and
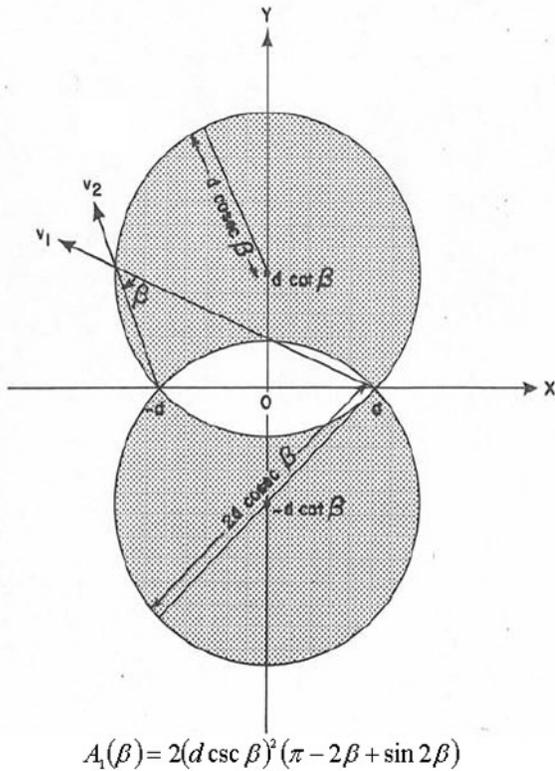
$$A_1(\beta) = 2(d\csc\beta)^2(\pi - 2\beta + \sin 2\beta)$$

Figure 15. Area A_1 that shows the dual-Doppler lobes as stippled areas. This area is bounded by the $\beta = 30°$) ($\pi/6$ rad) (Figure 1a in Davies-Jones, 1979).
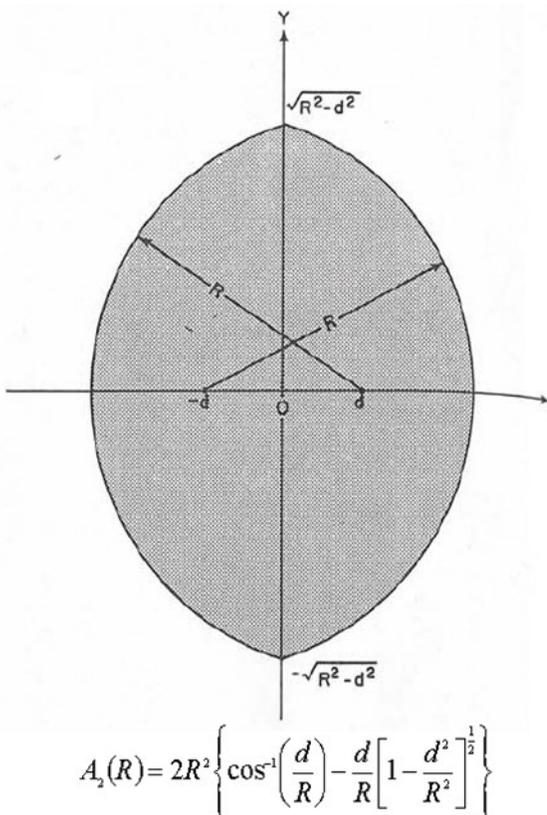

$$A_2(R) = 2R^2\left\{\cos^{-1}\left(\frac{d}{R}\right) - \frac{d}{R}\left[1 - \frac{d^2}{R^2}\right]^{\frac{1}{2}}\right\}$$

Figure 16. Area A_2, shown as a stippled area that lies within distance R of both radars (Figure 1b in Davies-Jones, 1979).

drawing changes that must occur to implement IRIS NDOP on a standalone basis.

NWS MLB Interests

NWS MLB agrees that the siting of the two radars is ideal for observing weather systems around KSC and CCAFS. Once the 45 WS and NWS MLB radar data co-exist for real-time dual-Doppler processing, NWS MLB can use the multi-sensor, multi-radar processing options via the Warning Decision Support System Integrated Information (WDSS-II) system for viewing. The WDSS-II is the second generation of a system of tools for the analysis, diagnosis and visualization of remotely sensed weather data. WDSS-II has the capability to merge multiple-radar data into four-dimensional grids including Terminal Doppler Weather Radar (TDWR) data. It is possible that both 45 WS radar data and TDWR data from MCO could be used to alleviate radar geometry issues at the NWS MLB radar, such as the cone of silence or beam blockage. In addition, in the event of a radar outage at one of the sites, the multi-radar algorithms would provide continuing coverage of the area through use of the data from the remaining operational radar sites.

Status

Dr. Huddleston completed the literature review and an outline of the final report. The next step is to calculate A_2 and A_{12}. She will gather more information from the 45 WS relating to the installation and costs of a data line to receive WSR-88D radar data from NWS MLB. Dr. Huddleston also began writing a draft of the final report.

For more information contact Dr. Lisa Huddleston at 321-853-8217 or lisa.l.huddleston@nasa.gov.
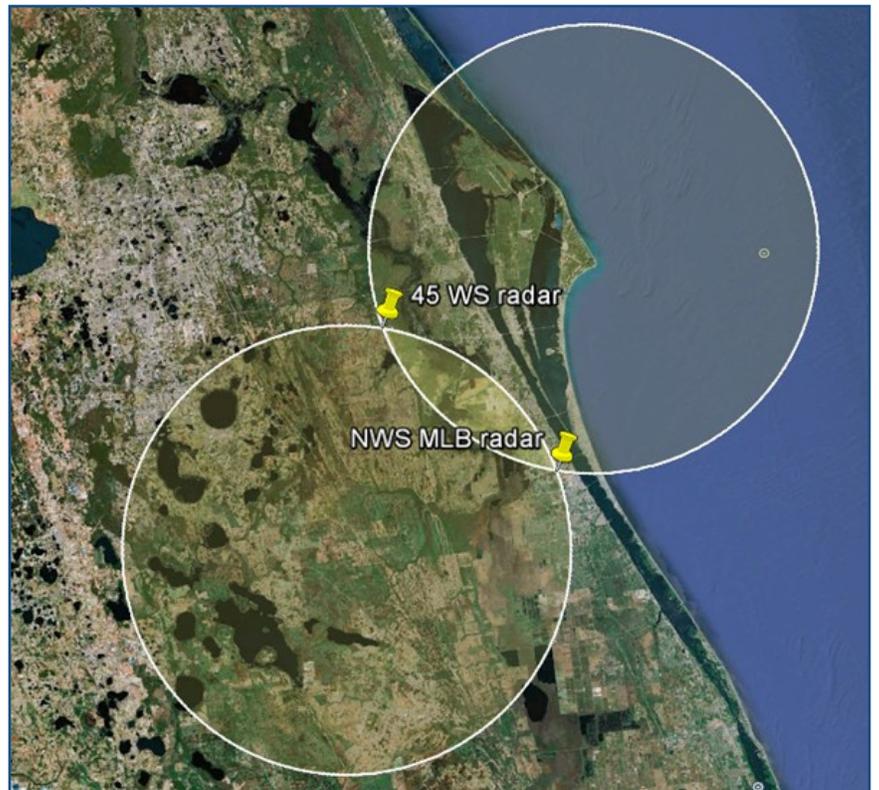
Figure 17. Area A_1 showing the dual-Doppler lobes of the 45 WS and NWS MLB radars. The yellow pins show the locations of the radars. The white circles are the dual-Doppler lobes within which the angles subtended by the radials from the radars lies between 30° and 150°. The intersecting area between the two circles along the radar baseline is not part of the dual-Doppler area because the beam crossing angles in this area are < 30° or > 150°.

MESOSCALE MODELING

Range-Specific High-Resolution Mesoscale Model Setup, Phase I (Dr. Watson)

The Eastern Range (ER) and Wallops Flight Facility (WFF) would benefit greatly from high-resolution mesoscale model output to better forecast a variety of unique weather phenomena. Global and national scale models cannot properly resolve important local-scale weather features at each location due to their horizontal resolutions being much too coarse. Therefore, a properly tuned model at a high resolution would provide that capability. This is the first phase in a multi-phase study in which the Weather Research and Forecasting (WRF) model will be tuned individually for each range. The goal of this phase is to tune the WRF model based on the best model resolution and run time while using reasonable computing capabilities. To accomplish this, the ER and WFF supported the tasking of the AMU to perform a number of sensitivity tests in order to determine the best model configuration for operational use at each of the ranges.

Phase I Details

The purpose of this phase is to choose the appropriate WRF model set-up and to ensure preliminary results are reasonable and similar to national model performance. In the first year of the task, Dr. Watson will compare output from the two WRF dynamical cores as well as physical parameterization settings within each core. She will run sensitivity tests to choose the most appropriate domain size, model run time, resolution, and nesting levels for each individual range. During the next phase in the following year, Dr. Watson will include observational data to initialize the model and test a number of different parameters within the data assimilation system. The WRF model is more likely to outperform various national models after this stage.

ER Grid Configuration

Dr. Watson installed the latest version of the WRF Environmental Modeling System (EMS) on the local AMU modeling cluster. The WRF EMS is a single end-to-end forecasting model that incorporates the two WRF dynamical cores in one system: the Advanced Research WRF (ARW) and the Non-hydrostatic Mesoscale Model (NMM). The software consists of pre-compiled programs that are easy to install and run operationally.

After installation, Dr. Watson ran different model configurations varying the dynamical core, grid spacing and domain size to determine the optimal configuration that allows for the largest domain size and highest resolution to capture unique weather phenomena on the ER with the shortest wall-clock run time. She determined two preliminary domain configurations for running the WRF model:

- Configuration 1: NMM core, 3 km outer domain and 1 km inner domain (WRF 3/1),

- Configuration 2: NMM core, 2 km outer domain and 0.67 km inner domain (WRF 2/0.6).

She chose the NMM core over the ARW core due to its significantly faster run-time. Dr. Watson will reevaluate these configurations after validating and comparing forecast results for the ER.

Running Test Cases

Dr. Watson began running test cases for the month of August 2011 to see if the model was able to capture the warm season convective initiation, onset of the seabreeze, and other warm season phenomena. A 9-hour forecast was run once per day starting at 1500 UTC for both domain configurations. The 12-km North American Mesoscale (NAM) model was used for boundary and initial conditions for both configurations.

Preliminary Results

Dr. Watson began validating WRF model forecasts with data from seven KSC/CCAFS wind towers. Two national models, the 13-km Rapid Update Cycle (RUC) and the NAM, were also validated against the same KSC/CCAFS wind towers in order to quantify the performance of the two WRF model forecasts versus that of the two national models. The purpose of this comparison was to ensure that the WRF forecasts were reasonable. It was not expected that the WRF would outperform the national models at this phase of the task for the reasons outlined at the bottom of the section.

Dr. Watson computed the monthly bias and root mean square error for wind speed, direction, temperature and dewpoint temperature for each model at select towers. Figure 18 shows preliminary results for wind speed and direction bias for August for the RUC, NAM and two WRF model configurations at the seven towers. The RUC model forecast of wind direction was the most accurate at the seven towers for August. The WRF 3/1 performed slightly, but not significantly, better than the WRF 2/0.6. The results for wind speed at the seven towers were more ambiguous, but the RUC and NAM consistently outperformed the two WRF configurations.

Figure 19 shows preliminary results for temperature and dewpoint temperature bias in August 2011 for the RUC, NAM and WRF configurations at five and four of the seven towers, respectively. Results were mixed for both the temperature and dewpoint temperature bias, with the WRF configurations slightly, but not significantly, outperforming the national models.

It is important to note some reasons why the RUC model performed better than the WRF configurations for the wind variables and had mixed results for the temperature variables:

- Dr. Watson did not use observational data to initialize the WRF model since it is not a requirement of this phase of the task,

- She used a 3-hourly forecast from the NAM for WRF initial and boundary conditions versus a 1-hourly forecast from the RUC since soil moisture and temperature data were not available in the archived RUC forecasts, and

- She did not use high-resolution Land Information System (LIS) or Sea Surface Temperature (SST) data in the WRF runs since archived LIS and high-resolution SST data were not available.

Dr. Watson will continue to validate the model performance of precipitation and will run WRF for the Florida cold season and compare results.

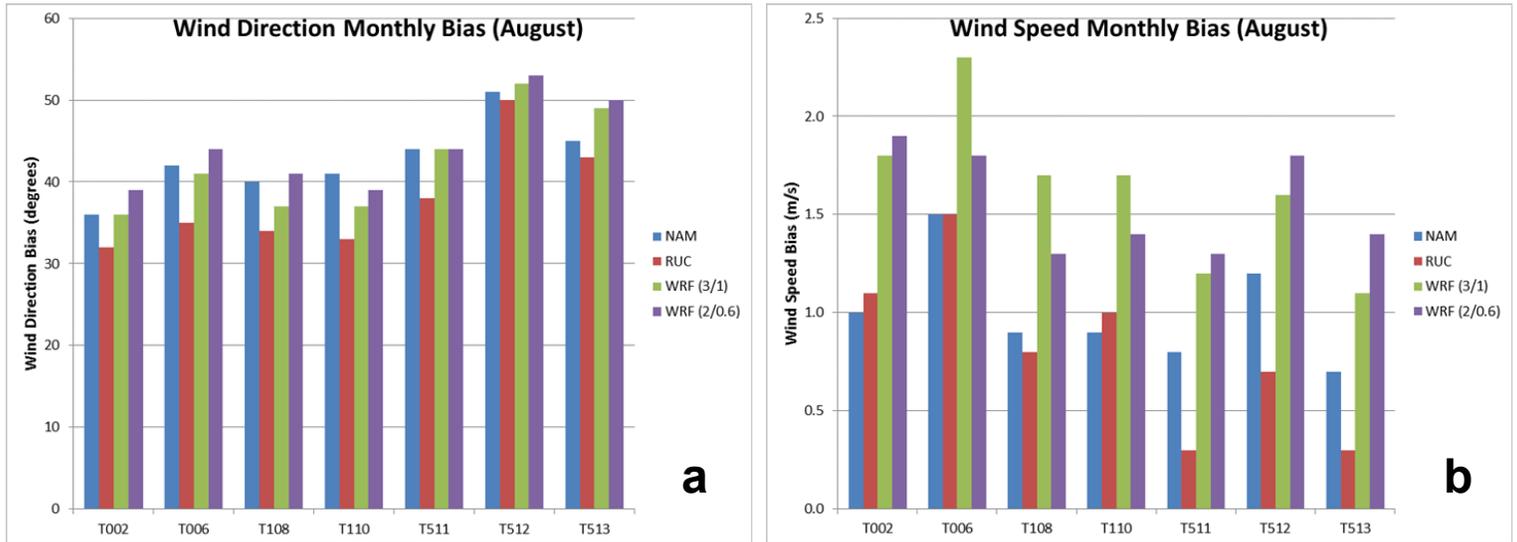For more information contact Dr. Watson at 321-853-8264 or watson.leela@ensco.com.

Figure 18. (a) Wind direction and (b) speed bias (m/s) in August 2011 at towers 2, 6, 108, 110, 511, 512 and 513 for the NAM, RUC, WRF 3/1 and WRF 2/0.6.
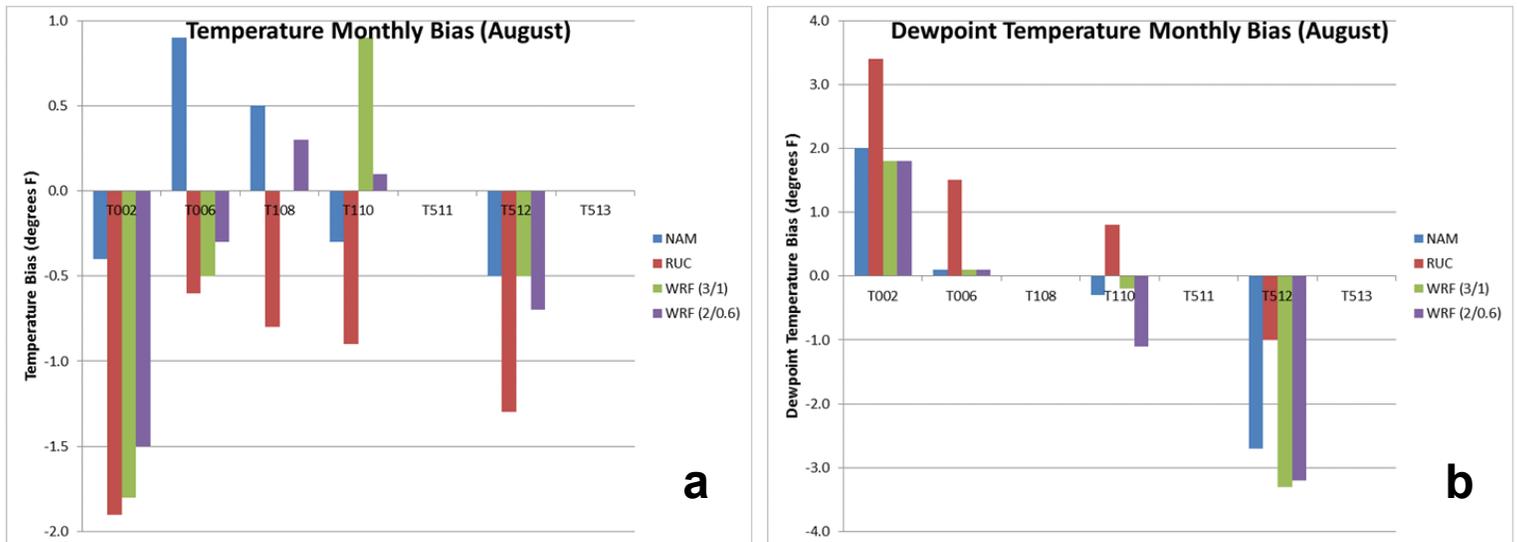
Figure 19. (a) Temperature (°F) bias at towers 2, 6, 108, 110 and 512 and (b) dewpoint temperature (°F) bias at towers 2, 6, 110 and 512 in August 2011 for the NAM, RUC, WRF 3/1 and WRF 2/0.6. .

AMU ACTIVITIES

AMU Chief's Technical Activities (Dr. Huddleston)

Dr. Huddleston, collaborating with Ms. Crawford, wrote an Excel program to calculate the correlation between flow regime and lightning occurrence changes for Mr. Roeder of the 45 WS. She used data from the Objective Lightning Probability Tool tasks discussed in this report. The correlation coefficients were low, indicating that a strong association between the two variables does not exist.

Dr. Huddleston and AMU team members developed a PowerPoint presentation outlining the purpose, operational product to develop, and customers for the current AMU tasks. Dr. Huddleston then presented it to the NASA/KSC Ground Processing Directorate management .

AMU Operations

As a cost saving measure, the AMU staff evaluated the overall computer hardware/operating system needs based on customer taskings, requirements and use of computer systems during the past few years. As a result of this evaluation, Mr. Wheeler turned in several computers, thereby reducing AMU computer overhead by 25%. The cost savings will be realized in reduced computer maintenance and IT security management.

Four AMU Windows 7 computers lost the ability to connect to the EN-SCO network. The cause appeared to be a conflict with a weekly Microsoft Windows software update and a security update from KSC IT to the AMU computers. Several helpdesk requests to the ENSCO and KSC IT departments could not solve the issue. Mr. Wheeler restored one computer with the Windows 7 operating system and the AMU's software suite, which restored the connection to the ENSCO network. He then developed an image of the computer's hard drive and restored it to the other three AMU computers.

To assist with AMU workload due to two AMU staff members' planned schedule changes, ENSCO, in coordination with the KSC Weather Office, hired Ms. Jaclyn Shafer to assist with AMU tasks on a part time basis. Ms. Shafer previously worked at NASA's Short-term Prediction Research and Transition Center in Huntsville, Ala.

REFERENCES

Armijo, L., 1969: A theory for the determination of wind and precipitation velocities with Doppler radars, *J. Atmos. Sci.*, **26**, 570-575.

Beck, J., 2004: High-resolution dual-Doppler analyses of the 29 May 2001 Kress, TX, cyclic supercell. M.S. thesis, Dept. of Geosciences, Atmospheric Sciences Group, Texas Tech University, 109 pp.

Bousquet, O., P Tabary, and J. du Châtelet, 2008: Operational multiple-Doppler wind retrieval inferred from long-range radial velocity measurements, *J. Appl. Meteor.*, **47**, 2929-2945.

Carey, L., 2005: Final progress report for the deployment of the C-band radars to DFW and HGB for the 2005 ozone season. Houston Advanced Research Center, Texas Environmental Research Consortium, 47 pp.

Davies-Jones, R., 1979: Dual-Doppler radar coverage area as a function of measurement accuracy and spatial resolution, *J. Appl. Meteor.*, **18**, 1229-1233.

Doviak, R. and D. Zrnic, 1993: *Doppler Radar and Weather Observations*. Academic Press, 562 pp.

Friedrich, K. and M. Hagen, 2004: On the use of advanced Doppler radar techniques to determine horizontal wind fields for operational weather surveillance. *Meteorological Applications*, **11**, 155-171, doi: 10.1017/ S1350482704001240.

Lambert, W. and M. Wheeler, 2005: Objective lightning probability forecasting for Kennedy Space Center and Cape Canaveral Air Force Station. NASA Contractor Report CR-2005-212564, Kennedy Space Center, FL, 54 pp. [Available from ENSCO, Inc., 1980 N. Atlantic Ave., Suite 830, Cocoa Beach, FL, 32931, and http://science.ksc.nasa.gov/amu/final-reports/objective-ltg-fcst-phase1.pdf.]

Lambert, W., 2007: Objective Lightning Probability Forecasting for Kennedy Space Center and Cape Canaveral Air Force Station, Phase II. NASA Contractor Report CR-2005-214732, Kennedy Space Center, FL, 57 pp. [Available from ENSCO, Inc., 1980 N. Atlantic Ave., Suite 830, Cocoa Beach, FL, 32931, and http://science.ksc.nasa.gov/amu/final-reports/objective-ltg-fcst-phase2.pdf.]

Lascody, R., 2002: The Onset of the Wet and Dry Seasons in East Central Florida – A Subtropical Wet-Dry Climate?, http://www.srh.noaa.gov/mlb/?n=wetdryseason.

Lhermitte, R. and L. Miller, 1970: Doppler radar methodology for the observation of convective storms. *14th Conf. on Radar Meteorology*, Tuscon, AZ, Amer. Meteor. Soc., 133-138.

NOAA, 2011: NOAA Central Library U.S. Daily Weather Maps Project, http://docs.lib.noaa.gov/rescue/dwm/data_rescue_daily_weather_maps.html.

O'Brien, J., 1970: Alternative solutions to the classical vertical velocity problem, *J. Appl. Meteor*., **9**, 197-203.

Rinehart, R., 2004: *Radar for Meteorologists*. 4th ed. Rinehart Publications, 482 pp.

TIBCO, 2010: TIBCO Spotfire S+® 8.2 Programmer's Guide, TIBCO Software Inc., Seattle, WA, 532 pp.

LIST OF ACRONYMS

14 WS	14th Weather Squadron
30 SW	30th Space Wing
30 WS	30th Weather Squadron
45 RMS	45th Range Management Squadron
45 OG	45th Operations Group
45 SW	45th Space Wing
45 SW/SE	45th Space Wing/Range Safety
45 WS	45th Weather Squadron
AFSPC	Air Force Space Command
AFWA	Air Force Weather Agency
AMPS	Automated Meteorological Profiling System
AMU	Applied Meteorology Unit
ARW	Advanced Research WRF
CCAFS	Cape Canaveral Air Force Station
CGLSS	Cloud-to-Ground Lightning Surveillance System
CSR	Computer Sciences Raytheon
EMS	Environmental Modeling System (WRF)
ER	Eastern Range
ESRL	Earth System Research Laboratory
FSU	Florida State University
FY	Fiscal Year
GSD	Global Systems Division
JSC	Johnson Space Center
KML	Keyhole Markup Language
KSC	Kennedy Space Center
LCC	Launch Commit Criteria
MCO	Orlando International Airport 3-letter identifier

MIDDS	Meteorological Interactive Data Display System
MLB	Melbourne International Airport 3-letter identifier
MSFC	Marshall Space Flight Center
NAM	12-km North American Mesoscale model
NCEP	National Centers for Environmental Prediction
NLDN	National Lightning Detection Network
NMM	Non-hydrostatic Mesoscale Model (WRF)
NOAA	National Oceanic and Atmospheric Administration
NWS MLB	National Weather Service in Melbourne, FL
PAFB	Patrick Air Force Base
POR	Period of Record
RRA	Range Reference Atmosphere
RUC	13-km Rapid Update Cycle
SMC	Space and Missile Center
TDWR	Terminal Doppler Weather Radar
USAF	United States Air Force
VAFB	Vandenberg Air Force Base
VBA	Visual Basic for Applications
WDSS-II	Warning Decision Support System Integrated Information
WFF	Wallops Flight Facility
WRF	Weather Research and Forecasting
WSR-88D	Weather Surveillance Radar 88 Doppler
XMR	CCAFS 3-letter identifier

The AMU has been in operation since September 1991. Tasking is determined annually with reviews at least semi-annually.

AMU Quarterly Reports are available on the Internet at http://science.ksc.nasa.gov/amu/.

They are also available in electronic format via email. If you would like to be added to the email distribution list, please contact Ms. Winifred Crawford (321-853-8130, crawford.winnie@ensco.com).

If your mailing information changes or if you would like to be removed from the distribution list, please notify Ms. Crawford or Dr. Lisa Huddleston (321-861-4952, Lisa.L.Huddleston@nasa.gov).

Distribution

NASA HQ/AA/
    W. Gerstenmaier
NASA KSC/AA/R. Cabana
NASA KSC/KT-C/J. Perotti
NASA KSC/LX/P. Phillips
NASA KSC/LX/S. Quinn
NASA KSC/LX-52/J. Amador
NASA KSC/NESC-1/S. Minute
NASA KSC/NE-D2-A/P. Nicoli
NASA KSC/GP/S. Kerr
NASA KSC/GP/D. Lyons
NASA KSC/GP/R. Mizell
NASA KSC/GP/P. Nickolenko
NASA KSC/GP-B/J. Madura
NASA KSC/GP-B/F. Merceret
NASA KSC/GP-B/
    L. Huddleston
NASA KSC/GP-B/J. Wilson
NASA KSC/GP-G4/R. Brown
NASA KSC/SA/R. Romanella
NASA KSC/SA/H. Garrido
NASA KSC/SA/B. Braden
NASA KSC/VA/A. Mitskevich
NASA KSC/VA-H/M. Carney
NASA KSC/VA-H1/B. Beaver
NASA KSC/VA-H3/
    P. Schallhorn
NASA KSC/VA-2/C. Dovale
Analex Corp/Analex-20/
    M. Hametz
NASA JSC/WS8/F. Brody
NASA MSFC/EV44/B. Roberts
NASA MSFC/EV44/R. Decker
NASA MSFC/EV44/H. Justh
NASA MSFC/ZP11/
    G. Jedlovec
NASA MSFC/VP61/J. Case
NASA MFSC/VP61/G. Stano
NASA WFF/840.0/R. Steiner

NASA WFF/840.0/A. Thomas
NASA WFF/840.0/T. Wilz
NASA DFRC/RA/E. Teets
NASA LaRC/M. Kavaya
45 WS/CC/S. Cahanin
45 WS/DO/B. Belson
45 WS ADO/W. Whisel
45 WS/DOR/M. McAleenan
45 WS/DOR/J. Smith
45 WS/DOR/M. Howard
45 WS/DOR/F. Flinn
45 WS/DOR/ T. McNamara
45 WS/DOR/J. Tumbiolo
45 WS/DOR/K. Winters
45 WS/DOR/D. Craft
45 WS/SY/M. Lewis
45 WS/SYA/J. Saul
45 WS/SYR/W. Roeder
45 RMS/CC/T. Rock
45 RMS/RMRA/R. Avvampato
45 SW/CD/G. Kraver
45 SW/SELR/K. Womble
45 SW/XPR/R. Hillyer
45 OG/CC/D. Sleeth
45 OG/TD/C. Terry
CSC/M. Maier
CSR 1000/S. Griffin
CSR 3410/C. Adams
CSR 3410/R. Crawford
CSR 3410/D. Pinter
CSR 3410/M Wilson
CSR 4500/J. Osier
CSR 4500/T. Long
SLRSC/ITT/L. Grier
SMC/RNP/M. Erdmann
SMC/RNP/T. Nguyen
SMC/RNP/R. Bailey
SMC/RNP(PRC)/K. Spencer

HQ AFSPC/A3FW/J. Carson
HQ AFWA/A3/M. Surmeier
HQ AFWA/A3T/S. Augustyn
HQ AFWA/A3T/D. Harper
HQ AFWA/16 WS/WXE/
    J. Cetola
HQ AFWA/16 WS/WXE/
    G. Brooks
HQ AFWA/16 WS/WXP/
    D. Keller
HQ USAF/A30-W/R. Stoffler
HQ USAF/A30-WX/
    C. Cantrell
HQ USAF/Integration, Plans,
    and Requirements Div/
    Directorate of Weather/
    A30-WX
NOAA "W/NP"/L. Uccellini
NOAA/OAR/SSMC-I/J. Golden
NOAA/NWS/OST12/SSMC2/
    J. McQueen
NOAA Office of Military Affairs/
    M. Babcock
NWS Melbourne/B. Hagemeyer
NWS Melbourne/D. Sharp
NWS Melbourne/S. Spratt
NWS Melbourne/P. Blottman
NWS Melbourne/M. Volkmer
NWS Southern Region HQ/"W/
    SR"/S. Cooper
NWS Southern Region HQ/"W/
    SR3"/D. Billingsley
NWS/"W/OST1"/B. Saffle
NWS/"W/OST12"/D. Melendez
NWS/OST/PPD/SPB/P. Roohr
NSSL/D. Forsyth
30 OSS/OSWS/DO/J. Roberts
30 OSS/OSWS/M. Schmeiser
30 OSS/OSWS/T. Brock
30 SW/XPE/R. Ruecker

Det 3 AFWA/WXL/K. Lehneis
NASIC/FCTT/G. Marx
46 WS//DO/J. Mackey
46 WS/WST/E. Harris
412 OSS/OSW/P. Harvey
412 OSS/OSWM/C. Donohue
UAH/NSSTC/W. Vaughan
FAA/K. Shelton-Mur
FSU Department of
    Meteorology/H. Fuelberg
ERAU/Applied Aviation
    Sciences/C. Herbster
ERAU/J. Lanicci
NCAR/J. Wilson
NCAR/Y. H. Kuo
NOAA/FRB/GSD/J. McGinley
Office of the Federal
    Coordinator for
    Meteorological Services
    and Supporting Research/
    R. Dumont
Aerospace Corp/T. Adang
ITT/G. Kennedy
Timothy Wilfong & Associates/
    T. Wilfong
ENSCO, Inc./J. Stobie
ENSCO, Inc./J. Clift
ENSCO, Inc./E. Lambert
ENSCO, Inc./A. Yersavich
ENSCO, Inc./S. Masters